

# THROUGH THE WALL IMAGING USING CHAOTIC MODULATED ULTRA WIDEBAND SYNTHETIC APERTURE RADAR

*Xiaoxiang Liu, Henry Leung*

Department of Electrical and Computer Engineering  
University of Calgary  
2500 University Drive NW  
Calgary, Alberta, Canada T2N 1N4

## ABSTRACT

A novel chaotic modulated ultra wideband (UWB) synthetic aperture radar (SAR) imaging scheme and its post data processing technique are presented for through the wall surveillance applications. It is illustrated that the proposed radar has an excellent resolution performance due to the autocorrelation properties of chaotic signals. Through modeling room reverberation and target reflection, and deriving energy distribution at the receiver, detection performance is carried out to show the advantages of proposed radar. Electromagnetic (EM) simulations are performed in a through the wall scenario. Compared with the conventional UWB radar, the result verifies the effectiveness and superiority of the proposed technique. Emails: {xiliu, leungh@ucalgary.ca}

**Index Terms**—Chaos, Synthetic Aperture Imaging, Ultra-Wide Band

## 1. INTRODUCTION

There has been a growing amount of interest in providing homeland security using reliable sensors recently. Among which include the demand for penetrating through walls, doors, and other opaque materials for perimeter monitoring of critical infrastructures and detecting unauthorized intrusion. Through the wall imaging technique has thus been brought forward in rescue missions, surveillance and reconnaissance [1,2]. Conventionally, Doppler radars are adopted for surveillance applications. However, they lead to a lot of false alarms in the presence of heavy clutters and thereby require a clear environment for operation. UWB signals possess the high spatial resolution that can be achieved due to very short pulses that characterize these signals. Although conventional time modulated UWB (TM-UWB) radar is used for high-resolution imaging, it suffers from poor sidelobe suppression characteristics, decreasing the effective range resolution and detection capability [3]. Extensive studies have shown that chaos

signals not only hold wideband nature with excellent range and Doppler resolution, but the richer dynamical structure of the chaos systems guarantees ease of generation, good spectrum controllability and sidelobe suppression.

In this paper, we present a chaotic modulated UWB SAR for through the wall surveillance purpose. Section 2 describes the proposed chaotic modulated UWB waveform and its SAR imaging techniques. Theoretical resolution and detection performance of proposed radar are discussed and compared in Section 3. As follows, post data processing technique is described and EM simulations are illustrated. Finally, conclusions are drawn in Section 5.

## 2. CHAOS MODULATED IMAGING TECHNIQUE

In this section, we propose a chaos based pulse amplitude modulated UWB (CPAM-UWB) noise waveform that will be applied in SAR imaging system.

### 2.1. Chaos modulated waveform

The transmitted CPAM-UWB signal can be given as

$$s(t) = \sum_{n=0}^{N-1} c_n \Omega(t - nT_d) \quad (1)$$

where  $c_n$  is the discrete chaotic waveform generated by a specific chaotic map. The basic UWB signal  $\Omega(t)$  can be chosen as the Gaussian pulse waveform

$$\Omega(t) = A \exp(-4\pi(t/\Delta T)^2) \quad (2)$$

with the peak amplitude  $A$  and the effective duration  $\Delta T$ .  $T_d$  in Eq. (1) refers to the pulse repetition interval (PRI).

### 2.2. Coherent SAR imaging

The received waveforms contain two types of signals, namely early time content and late time content. The former is dominated by antenna coupling and reflections from the wall. The latter is mainly composed of target propagation and reflections from clutter. The filtering techniques are first

applied to remove the early time content. In this stage, care should be taken not to remove the reflections due to targets lying close to the wall. Here, each point in the 2-D location is treated as a focal point and assigned an intensity value [4]. The round trip distances from the antenna positions to the focal point are converted into delays. Consider a single transmitter/receiver pair moving around the building, formed an M-element array. The position of the  $m^{\text{th}}$  transmitting and receiving antennas is  $(x_{tm}, y_{tm})$  and  $(x_{rm}, y_{rm})$ , respectively. Assume that  $(x_p, y_p)$  represents the position of the target whose complex reflectivity of the point target is  $\sigma_p$ . See Figure 1. The received signal at the  $m^{\text{th}}$  antenna can be expressed by

$$r_m(t) = \sigma_p s(t - \tau_m) \quad (3)$$

where  $\tau_m$  is the round trip time delay.

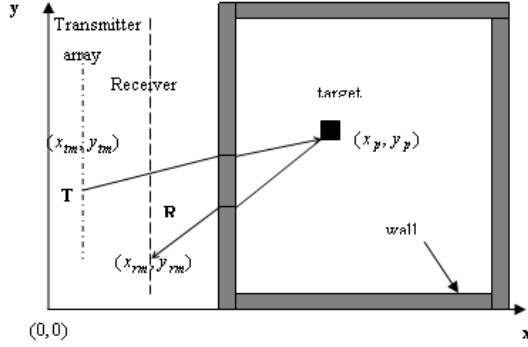


Figure 1. Geometry of target and wall

The intensity of the radar image at the focal point  $(x, y)$ ,  $I(x, y)$  is given by coherently summing the reflected signals. That is,

$$I(x, y) = \left[ \sum_{m=1}^M r_m(\tilde{\tau}_m) \right]^2 \quad (4)$$

where  $M$  denotes the total number of location where transmitter/receiver pair locates.  $\tilde{\tau}_m$  is the estimated delay experienced by  $r_m(t)$  for a signal  $s(t)$  transmitted from  $(x_{tm}, y_{tm})$  to  $(x, y)$  and then back to  $(x_{rm}, y_{rm})$ . The process is performed for all points in the region of interest to generate the composite image of the scene. The general case of multiple targets can be obtained by superimposing all target reflections.

### 3. PERFORMANCE ANALYSIS

#### 3.1. Resolution performance

The received radar signal is convolved with a matched filter impulse response to analyze the resolution performance of the proposed modulation scheme, which is essentially the process of ambiguity function [5]. The temporal resolution  $\Delta\tau$  is taken as the delay beyond which

the ambiguity function drops below  $2/3$  of the peak value of the ambiguity function  $\chi(0,0)$ , that is,  $\Delta\tau = \chi^{-1}(2\chi(0,0)/3)|_{v=0}$  as a consequence. The above inverse function was experimentally evaluated for a range of  $\Delta\tau$  and the resulting curve was fitted using closed form functions. The resulting range resolution is shown in Fig. 2. It can be observed that the resolution of chaos modulated signal is better than the TM-UWB radar for a given bandwidth.

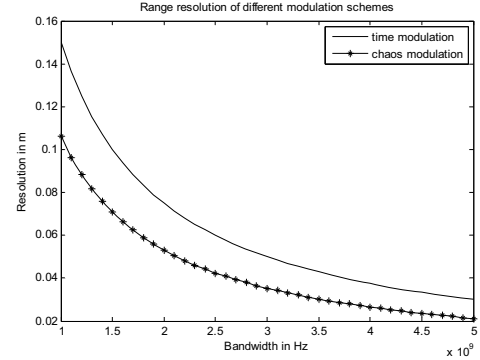


Figure 2. Range resolution of different modulation schemes

#### 3.2. Detection performance

The detection bound of a through-the-wall sensing system depends on the dielectric nature of the targets, walls, their geometry and the transmitted signal characteristics. The transmitted chaotic modulated UWB pulses pass through a wall penetration radar channel. Mathematically, the convolved signal can be written using output error model as:

$$\begin{aligned} x_n &= \mathbf{a}^T x_{n-1} + \mathbf{h}^T c_n \\ r_n &= x_n + w_n \quad (n = 0, \dots, N-1) \end{aligned} \quad (5)$$

Where  $r_n$  is sampled version of the received signal,  $\mathbf{a}^T$  is an autoregressive (AR) coefficient vector that models wall reverberation,  $\mathbf{h}^T$  is a moving average (MA) coefficient vector that models target reflections,  $c_n$  is the driven chaotic signal generated by 1-D chaotic map  $c_n = f(c_{n-1})$ ,  $x_n$  is the filtered signal vector and  $w_n$  is a realization of a white Gaussian noise process with a variance of  $\sigma_w^2$ . The radar estimates the signal energy at different delays hence detecting and ranging various targets.

Let  $s(t)$  be the CPAM-UWB transmitted signal. Maxwell's wave propagation equations are solved to obtain the received signal due to a target with dielectric constant  $\epsilon_t$  at a distance  $D$  from the radar. Let  $E_t = \int s^2(t) dt$  be the transmitted signal energy, and  $\Gamma$  be the transmission factor of the dielectric wall. For a homogeneous non-magnetic dielectric medium such as wooden or concrete

walls, the transmission factor  $\Gamma$  depends only on the dielectric constant of the wall material  $\epsilon_w$ , the polarization of the transmitted signal and the angle of incidence,  $\theta$ . However, this value relies on the antenna polarization.

For perpendicular polarization, the electric field is parallel to the reflecting surface. By the continuity of the tangential component of the electric field and the law of conservation of signal energy we have

$$\Gamma = 1 + \frac{\cos \theta - \sqrt{\epsilon_w - \sin^2 \theta}}{\cos \theta + \sqrt{\epsilon_w - \sin^2 \theta}} \quad (6)$$

For parallel polarization, the magnetic field is parallel to the reflecting surface. By the same principles as Eq. (6),  $\Gamma$  becomes

$$\Gamma = 1 + \frac{\epsilon_w \cos \theta - \sqrt{\epsilon_w - \sin^2 \theta}}{\epsilon_w \cos \theta + \sqrt{\epsilon_w - \sin^2 \theta}} \quad (7)$$

When the transmitter is parallel polarized, for a particular angle of incidence,  $\theta = \tan^{-1} \sqrt{\epsilon_t}$ , there is no reflection from the wall and all the energy in the signal get completely transmitted.

The re-radiated signal from the target gets scaled by a factor corresponding to the radar cross section (RCS),  $\sigma$  of the target. For nonmagnetic targets, with linear dimensions of  $L \times W$  and an orientation of  $\psi$  with respect to the horizontal, the RCS can be expressed as

$$\sigma = LW \sin \psi \frac{1 - \sqrt{\epsilon_t}}{1 + \sqrt{\epsilon_t}} \quad (8)$$

Thus the effective received signal energy at a collocated isotropic radar receiver due to target at a distance  $D$  from the radar is given by

$$E_r(\epsilon_w, \epsilon_t, D) = E_t \Gamma^2 \frac{1}{16\pi^2 D^4} LW \sin \psi \frac{1 - \sqrt{\epsilon_t}}{1 + \sqrt{\epsilon_t}} \quad (9)$$

It can be shown that for building with large rooms, the AR coefficient is a function of the room's linear dimensions.

$$E_w = E_t \Gamma^2 \left[ \Omega + \Omega^2 + \dots \right] \quad (10)$$

where  $\Omega$  is the AR coefficient. We therefore have

$$E_w = E_t \Gamma^2 \Omega \frac{1}{1 - \Omega} \quad (11)$$

In the absence of target with the return energy  $E_w$ , The received energy follows Rician distribution which is given by

$$P(E|0) = \frac{E}{\sigma_w^2} e^{-\frac{(E^2 + E_w^2)}{2\sigma_w^2}} I_0 \left( \frac{E E_w}{\sigma_w^2} \right) \quad (12)$$

In the presence of target with the return energy  $E_r + E_w$ , the conditional distribution of the received energy is given by

$$P(E|1) = \frac{E}{\sigma_w^2} e^{-\frac{(E_r + E_w)^2 + E^2}{2\sigma_w^2}} I_0 \left( \frac{(E_r + E_w)E}{\sigma_w^2} \right) \quad (13)$$

We simulated a room scenario with wooden walls and single target for CPAM-UWB radar and TM-UWB radar. The ROC curve is shown in Fig. 3 to illustrate the detection performance of the two schemes. It can be seen that the thinner the wall is, the better detection performance the radar will achieve. Furthermore, the proposed CPAM-UWB radar obtains a better detection performance than conventional TM-UWB radar.

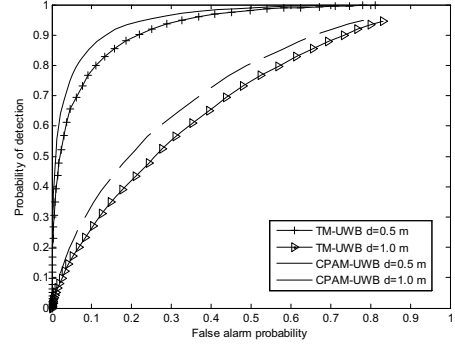


Figure 3. Detection performance of CPAM-UWB and TM-UWB radar

## 4. SIMULATIONS

### 4.1. Motion compensation

In through the wall UWB SAR imaging system, the radar platform usually can not precisely follow a straight and constant line, which will result in the loss of geometric resolution, reduction of image contrast and hence reduced detection performance. Motion compensation technique built into the design of image processing is therefore essential in SAR imaging process. In this paper, we apply a motion compensation algorithm developed in [6], which proves to be effective in compensating for deviations from a straight moving path. The main idea of the this method is to combine wavenumber domain processing with a procedure that enables motion compensation to be applied as a function of target range and azimuth angle. In implementation, we assume that the radar beamwidth is 1 radian and the radar is operated beyond  $x$  m. For complete coverage, the radar should be such that its beamwidth reaches all areas of the front wall. Suppose  $d$  is the length of the front wall in m, and the antenna beamwidth is fixed at  $\theta$  radians, the antenna should be operated at  $\tan \frac{\theta}{2} = \frac{d}{2x}$  for maximal coverage. Usually for UWB antennas, in order to have azimuthal resolution comparable to that of range resolution of 1 radian,  $x = 0.915d$  m. The simulation

configurations and its results will be demonstrated as follows.

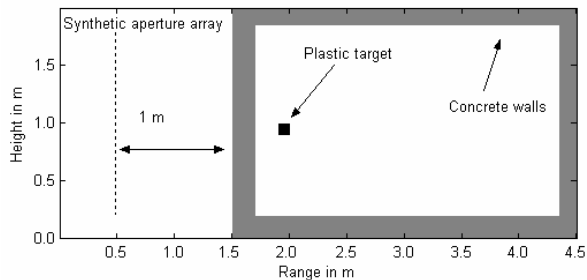


Figure 4. Simulation setup

## 4.2. Simulation results

Here, we perform the finite difference time domain (FDTD) numerical simulation for SAR imaging exploiting the proposed CPAM-UWB waveform and post data processing techniques. The simulation scenario is illustrated in Fig. 4. A single target ( $\epsilon = 3$ ) is placed 0.5 m behind the front wall ( $\epsilon = 6$ ). The synthetic aperture array platform, composed of a transmitter/receiver pair, is located 1m away from the front wall and moves along a straight path. As the result, 21 array locations are formed to capture the EM waves reflected from the region of interest. In transmitter settings, a Gaussian pulse was applied to simulate the antenna with a center frequency of 1 GHz. 1-D Chebyshev map is used to modulate the amplitude of the Gaussian pulse. Fig 5 and Fig 6 represent images of target after filtering wall reverberations and motion compensation, formed by CPAM-UWB radar and TM-UWB radar respectively. It can be seen clearly that the proposed CPAM-UWB based SAR has better sidelobe clutter suppression and thus reveals good performance in recognizing the target in heavy clutter situation.

## 5. CONCLUSION

We offer a novel chaotic modulated UWB waveform and a coherent SAR based imaging technique. The wide spectral nature as well as the excellent autocorrelation property of chaotic signal enables good resolution and detection performance of the proposed scheme. Motion compensation problem is also considered in this paper to enhance the imaging performance. Numerical EM through the wall simulations in a closed environment confirm the theoretical analysis.

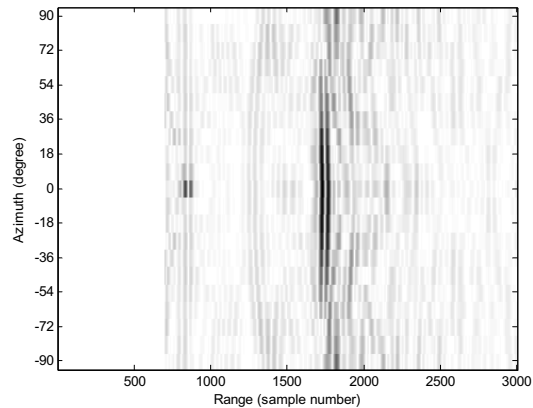


Figure 5. Detection performance of CPAM-UWB radar

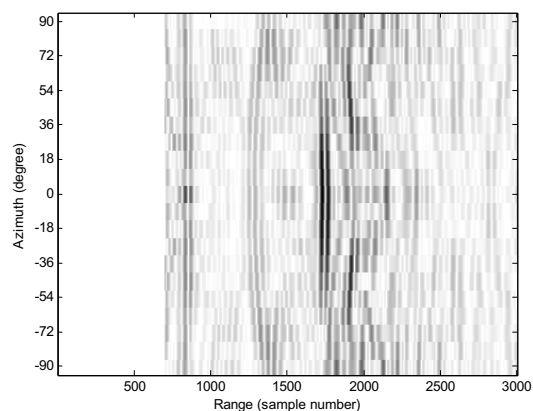


Figure 6. Detection performance of TM-UWB radar

## 6. REFERENCES

- [1] F. Ahmad, M. G. Amin, S. A. Kassam, "Synthetic aperture beamformer for imaging through a dielectric wall", IEEE transactions on aerospace and electronic systems. vol. 41, no.1, pp. 271-283, 2005
- [2] P. Withington, H. Fluhler, and S. Nag, "Enhancing homeland security with advanced UWB sensors", IEEE microwave magazine, no. 3, pp. 51-58, Sept. 2003
- [3] S. Nag, H. Fluhler, and M. Barnes, "Preliminary interferometric images of moving targets obtained using a time-modulated ultra-wideband through-wall penetration radar", Proceedings of IEEE Radar Conference, pp. 64-69, 2001
- [4] B. Juhel, E. Legros, and M. Le Goff, "Algorithms and experimental results in ultra-wideband SAR imaging", Radar 97 (Conf. Publ. No. 449), pp. 673-677, Oct. 1997
- [5] S. Stein, "Algorithm for ambiguity function processing", IEEE transaction on acoustics, speech, and signal processing, vol. ASSP-29, no. 3, pp. 588-599, June 1981
- [6] S.N. Madsen. "Motion compensation for ultra wide band SAR", IGARSS' 2001, International Geoscience and Remote Sensing Symposium, vol. 3, 1436 – 1438, 9-13 July 2001